Overcoming Multidrug Resistance in Microbials Using Nanostructures Self-Assembled from Cationic Bent-Core Oligomers

Shao Qiong Liu, Shrinivas Venkataraman, Zhan Yuin Ong, Julian M. W. Chan, Chuan Yang, James L. Hedrick, and Yi Yan Yang**

The emergence of drug-resistant microbes and the shortage of new antibiotics constitute severe threats to human health worldwide.[1] For instance, in the United States, methicillin-resistant *Staphylococcus aureus* (MRSA, Gram-positive) is the most common drug-resistant bacterium and accounts for 52% of nosocomial infections in intensive care units.[2] It causes surgical site infections, bacteremia and pneumonia, and is responsible for significant morbidity and mortality.[3] As a consequence, there is an urgent need for the development of novel antimicrobial agents to treat infectious diseases, especially those caused by multidrug-resistant (MDR) microbes.

In response to infections by pathogenic microbes, nearly every multicellular organism secretes short cationic amphiphilic peptides that possess host-defense properties, known as antimicrobial peptides (AMP).[4] Owing to the unusually broad spectrum of activities against Gram-negative and Gram-positive bacteria, viruses, fungi and other parasites, the potential therapeutic use of AMP as anti-infective agents has been exploited. The co-presence of positively-charged groups (hydrophilic) and hydrophobic components on AMPs allows the macromolecules to adopt facially amphiphilic conformations.[5] Cationic residues are key for enabling electrostatic interaction with negatively-charged bacterial membranes, while the hydrophobic side chains are critical for subsequent insertion into these lipid-based membranes, ultimately causing membrane disintegration and cell death by lysis.[6] The physical nature of this antimicrobial mechanism makes it difficult for bacteria to develop resistance to AMPs. In contrast, conventional antibiotics usually target specific biochemical pathways within the pathogenic bacteria, thus the likelihood of drug resistance stemming from genetic mutation is much greater. On the other hand, the cytotoxicity, poor in vivo stability, and the high production costs associated with AMPs have precluded their use in clinical applications.[7] To address these issues, several synthetic polymers have been designed to mimic the amphiphilicity and antimicrobial activity of AMPs. For example, cationic derivatives of poly(arylamide),[8] poly(methacrylate),[9] poly(ethyleneimine),[10] poly(norbornene),[11] poly(β-lactam),[12] pyridinium-based polymers[13] and synthetic polypeptides (made from *N*-carboxyanhydrides)[14] have demonstrated comparable antimicrobial activities against different strains of bacteria, with cell membrane disruption being the common mode of action in all cases. While these synthetic analogs are relatively easy and inexpensive to prepare in bulk, it remains challenging to design polymers having both potent antimicrobial activity and high selectivity towards microbes (i.e., not toxic to mammalian cells).

Recently, we reported several biodegradable and biocompatible cationic amphiphilic polycarbonates that self-assembled into cationic micellar nanoparticles.[15] These nanoparticles displayed potent antimicrobial activities against fungi and Gram-positive bacteria including MRSA. By fine-tuning the hydrophilicity/hydrophobicity balance, polycarbonate homopolymers with optimal compositions achieved strong activity against both Gram-positive and Gram-negative bacteria with negligible toxicity toward mammalian cells.[15,17] Herein, we report the synthesis, self-assembly and antimicrobial activity of a series of novel oligomeric cationic compounds of discrete molecular weights. These compounds were designed with a rigid hydrophobic terephthalamide-bisurea core flanked by hydrophilic imidazolium groups with short alkyl (C_nH_{2n+1}, n<6) or simple aryl tails, and were found to readily self-assemble into nanostructures in aqueous solutions. The cationic oligomer with optimal hydrophobic/hydrophilic balance showed potent, broad-spectrum antimicrobial activity and high selectivity towards Gram-positive bacteria (including clinically-isolated MRSA), killing the microbes via the membrane-lytic mechanism. Furthermore, the bacteria failed to develop drug resistance even after multiple exposures to sub-lethal doses of the compound.

The key design element of our cationic antimicrobial oligomers is based on the rigid terephthalamide core generated via the organocatalytic aminolysis of poly(ethylene terephthalate) (PET) with 4-aminobenzylamine and

Dr. S. Q. Liu, Dr. S. Venkataraman, Dr. Z. Y. Ong, Dr. C. Yang, Dr. Y. Y. Yang
Institute of Bioengineering and Nanotechnology
31 Biopolis Way, The Nanos
Singapore 138669, Singapore
E-mail: yyyang@ibn.a-star.edu.sg
Dr. J. M. W. Chan, Dr. J. L. Hedrick
IBM Almaden Research Center
650 Harry Road, San Jose, CA 95120, USA
E-mail: hedrick@us.ibm.com

DOI: 10.1002/smll.201303921

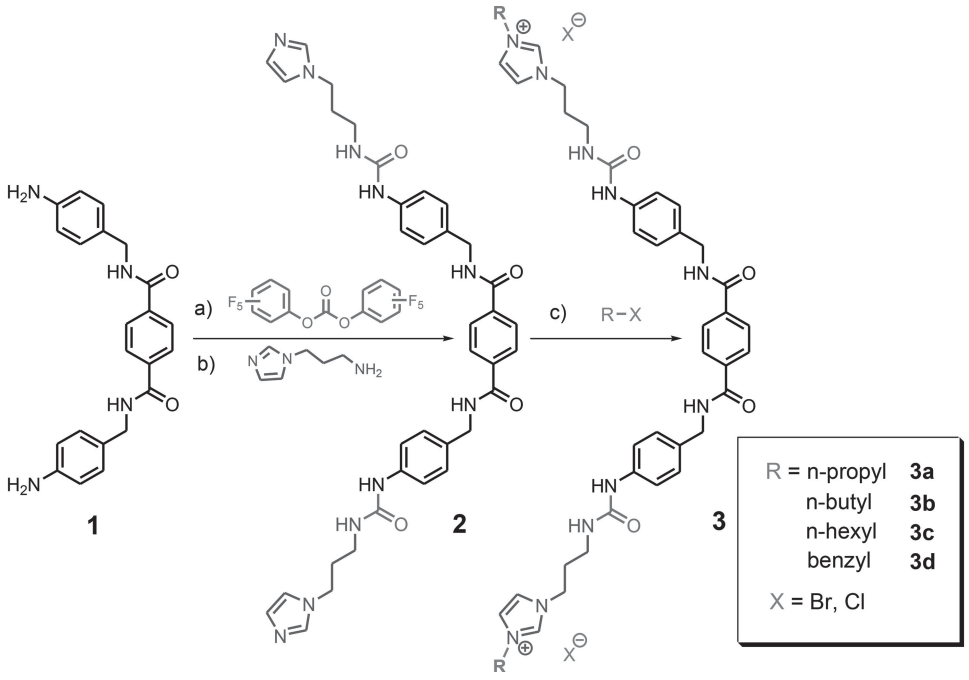

Scheme 1. Synthesis of compounds **3a-d.**

1,5,7-triazabicyclo[4.4.0]dec-5-ene (TBD). The resulting diamine was reacted with bis(pentafluorophenyl)carbonate to generate a reactive carbamate intermediate, which was subsequently treated with 1-(3-aminopropyl)imidazole to afford a bis-urea derivative with terminal imidazole moieties. The imidazoles were quaternized via alkylation with propyl-, butyl-, hexyl-, and benzyl- halides to generate four cationic compounds with molecular weights ranging from 843.0 to 927.1 g/mol (**Scheme 1** and Supporting Information Table S1). The syntheses of these compounds are detailed in the Supporting Information along with their characterization data. Interestingly, the complementary hydrogen bonding motifs present within the rigid-rod terephthalamide-bisurea oligomers facilitate self-assembly in aqueous solutions to afford supramolecular structures. Moreover, the placement of the charge relative to the hydrophobic component resembles the "same-centered" antimicrobial design approach where both the charged and hydrophobic components are in proximity within the same repeat unit. This approach has been shown to be effective in achieving potent bacterial membrane-lysing activity while mitigating undesirable toxicity.[16,17]

In water, the cationic oligomers were able to self-assemble into supramolecular nanostructures with critical micelle concentrations (CMCs) ranging from 30 to 80 mg/L (12–60 mg/L in tryptic soy broth (TSB)-bacterial culture media) and zeta potentials of 29.9–44.5 mV (**Table 1**). The respective CMCs are dependent on the hydrophobicity of the terminal alkyl/aryl tails, with increased hydrophobicity (from **3a** to **3c**) giving lower CMC values. Dissolution of compounds **3a** through **3c** in water gave self-assembled nanostructures of different shapes, sizes, and morphologies (**Figure 1**). Compound **3a** formed long and flexible nanofibers with a diameter of ≈5 nm and a length of ≈ 1 μm (Figure 1a). Molecular mechanics conformational analysis revealed that terephthalamide-bisurea core adopted a zigzag or bent structure.[18] Self-assembly of the cores via urea-urea hydrogen bonds and π–π stacking interactions resulted in flat, sheet-like superstructures. Mutual stacking of these planar sheets in turn gave rise to a multilayer nanofiber stabilized by intermolecular hydrogen bonding, π–π stacking and hydrophobic interactions. The extra carbon in each of the terminal alkyl tails of **3b**

Table 1. Physico-chemical properties and antimicrobial activity of small cationic compounds.

Cationic Compounds	M_w	CMC [mg/L]	Zeta potential [mV]	SI[b)]	MIC [mg/L]					
					S.E[c)]	*S. aureus 6538*	*S. aureus 29737*	*MRSA*	*E. coli*	*C. A*[d)]
3a	843.0	80 (60)[a)]	29.9 ± 1.4	>10.0	250.0	250.0	250.0	250.0	>500.0	250.0
3b	871.0	60 (25)	38.2 ± 0.5	>20.0	125.0	125.0	125.0	125.0	500.0	125.0
3c	927.1	30 (12)	40.3 ± 0.9	64.1	15.6	15.6	15.6	15.6	250.0	62.5
3d	894.5	40 (12)	44.5 ± 1.4	64.1	15.6	31.2	31.2	15.6	250.0	125.0

[a)]Measured in TSB; [b)]Selectivity index (SI) is calculated as HC_{15}/MIC_{MRSA}, where HC_{15} was defined as the lowest concentration that induces >15% hemolysis and MIC_{MRSA} was defined as the MIC of compounds against MRSA; [c)]*Staphylococcus epidermidis*; [d)]*Candida albicans*

small 2014,
DOI: 10.1002/smll.201303921

NANO MICRO small

instead gave rise to short and stiff nanorods with diameters of ≈5 nm and lengths of under 300 nm (Figure 1b). It is possible that the presence of longer alkyl chains disrupts the delicate balance of intermolecular forces needed for nanofiber assembly. With compounds **3c** and **3d**, featuring hexyl and benzyl tails, spherical nanostructures with an average diameter of 10 and 28 nm were formed, respectively (Figure 1c,d). These observations suggest that hydrophobic tail length and/or composition of the cationic oligomers play a crucial role in determining the architectures of the resulting self-assembled nanostructures.

The antimicrobial activity of the cationic compounds were evaluated against clinically relevant microorganisms, including *S. epidermidis, S. aureus* and clinically isolated MRSA (Gram-positive), *E. coli* (Gram-negative), and *C. albicans* (yeast). As shown in Table 1 and Supporting Information Figure S1, the cationic compounds with optimal compositions showed broad-spectrum antimicrobial activity against all the microorganisms tested with low minimum inhibitory concentrations (MICs). Compounds **3a** and **3b** featuring shorter terminal alkyl chains did not show strong antimicrobial activity, but when the chain length was increased to 6 carbon atoms (i.e., **3c**), the antimicrobial activity became remarkably enhanced. This is likely due to an increased propensity of the hydrophobic chains to intercalate and disrupt the bacterial membranes. Compound **3d** displayed similar antimicrobial activity compared to **3c**, consistent with the increased hydrophobicity conferred by the benzyl group. Thus, the results suggested that an appreciable degree of hydrophobicity in the tails was required for activity against the microbes. In addition, the cationic compounds were also found to be more active against Gram-positive bacteria than Gram-negative bacteria (Table 1). This was unsurprising considering the presence of an additional outer membrane in Gram-negative bacteria.[19] The membrane of Gram-negative bacteria consists of a small amount of anionic phosphatidylglycerol (PG) and mostly of zwitterionic phosphatidylethanolamine (PE), whereas that of Gram-positive bacteria is rich in anionic lipids such as PG and cardiolipin (CL).[20] Therefore, Gram-negative bacteria may show diminished affinity for our cationic compounds, and the installation of additional hydrophobic moieties may be needed for the permeation and disruption of these lipid bilayers. It is worthy noting that the MICs of the cationic compounds were above their CMC values in microbial culture media (Table 1), suggesting that the formation of nanostructures was necessary for antimicrobial activity. This finding is consistent with our previous observations that self-assembled nanostructures from amphiphilic triblock polycarbonate copolymers and cationic short peptide (CG3R6TAT-cholesterol conjugate) had strong microbicidal activity against Gram-positive bacteria.[15,21] In addition, from our recent study,[18a] nanofibers and spherical nanoparticles had similar potency against microbes. The discrepancy in antimicrobial activity between these compounds was likely because of their hydrophobicity. Importantly, the nanostructures arising from relatively more hydrophobic **3c** (hexyl tail) and **3d** (benzyl tail) showed strong antimicrobial activity especially against Gram-positive bacteria.

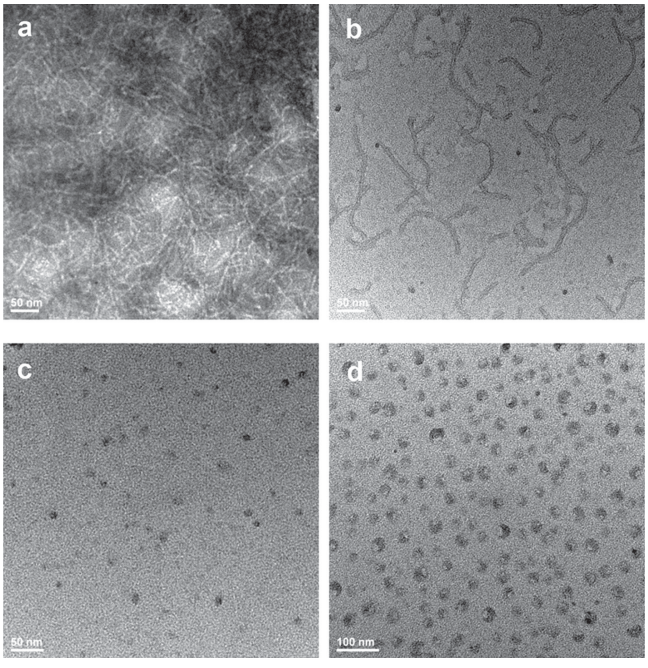

Figure 1. TEM images of small cationic compounds by direct dissolution in water at 1000 mg/L. a) 3a; b) 3b; c) 3c, and d) 3d.

Microbicidal properties of the cationic compounds were evaluated by measuring the viability of microbial cells incubated with these compounds at various concentrations. As shown in **Figure 2**a and Supporting Information Table S2, for the microorganisms tested, compounds achieved more than 3 log and 5 log reductions in colony counts at their respective MIC and 2×MIC values respectively, implying that these compounds were microbicidal. Overall, **3c** exhibited superior antimicrobial activity, and was therefore selected for further studies.

Microbial killing kinetics of **3c** was investigated by quantifying the viable colonies at specific time intervals upon treatment at MIC and 2×MIC concentrations. *S. aureus* 29737 and *E. coli* were chosen as model microorganisms. The compound **3c** showed a dose-dependent rapid microbicidal effect (Figure 2b). The killing rate was enhanced at 2×MIC as compared to MIC. More than 99.9% (>3 log reduction in colony) of *S. aureus* cells were killed by **3c** after 3 h of exposure to 2×MIC, with complete eradication after 6 h. It was observed that **3c** killed *E. coli* much faster than it did *S. aureus* despite having higher MICs. It reduced the viable count of cells by more than 99.9% within 30 min and eliminated the cells completely after 90 min at 2×MIC (Supporting Information Figure S2).

To assess the possibility of bacterial resistance against our cationic compounds, microbial cells were exposed to **3c** multiple times at a sub-lethal concentration (1/8 of MIC).[22] The conventional antibiotic penicillin G was used as the control. An increasing MIC was observed for penicillin G against *S. aureus* 29737 as a function of the number of exposures (Figure 2c). Similar observations were also reported by Suskovic et al.[23] On the contrary, repeated treatments with **3c** did not lead to an increase in MIC, indicating that **3c** did not induce any drug-resistance over the course of study.

To understand the antimicrobial mechanism of the cationic compounds, field emission scanning electron

DOI: 10.1002/smll.201303921

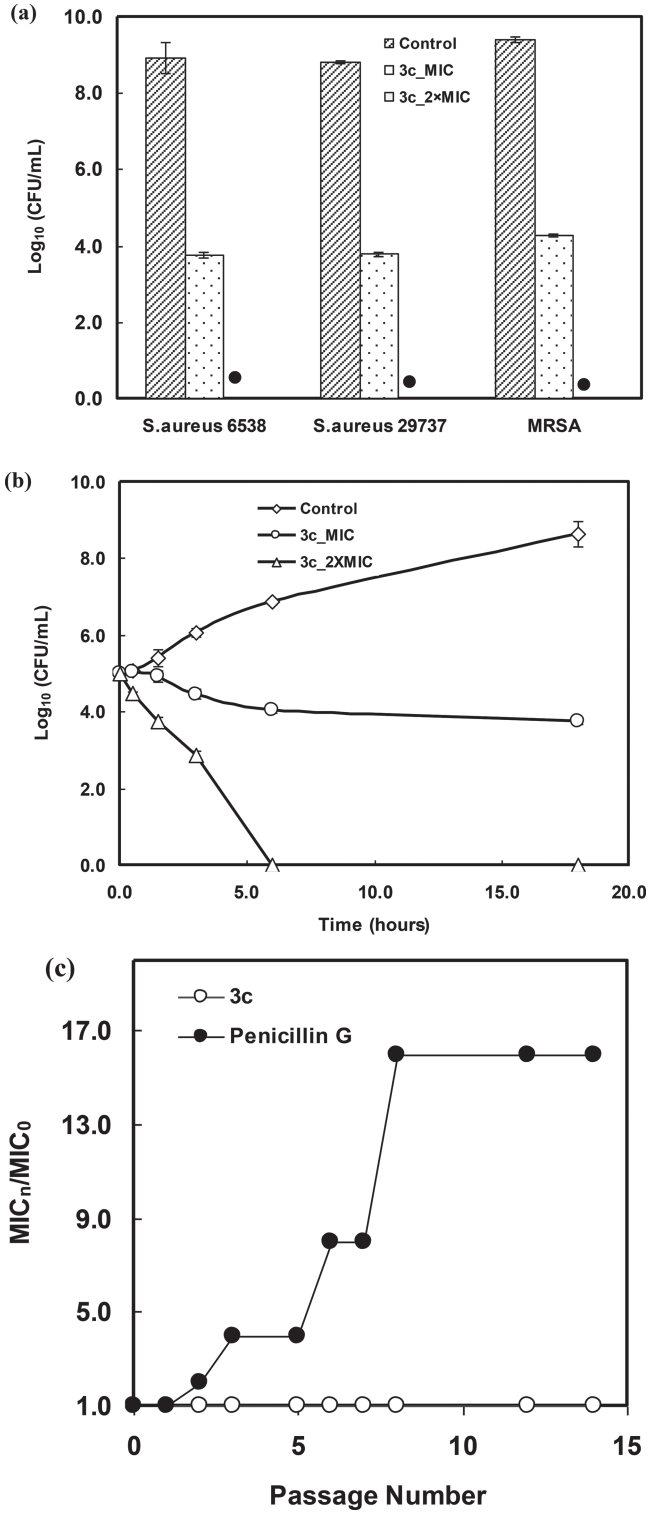

Figure 2. Antimicrobial activity of cationic compound 3c against various microbes and evaluation of drug resistance. a) Colony formation units (CFUs) of various *S. aureus* strains after treated with 3c at MIC and 2×MIC for 18 h (· denotes the absence of any observed colony); b) CFUs of *S. aureus* 29737 after incubation with 3c for various periods of time; c) Changes in MIC of antimicrobial agents against *S. aureus* 29737 upon multiple sub-lethal dose exposures.

microscopy (FE-SEM) was employed to visualize the morphological changes of bacteria before and after treatment with

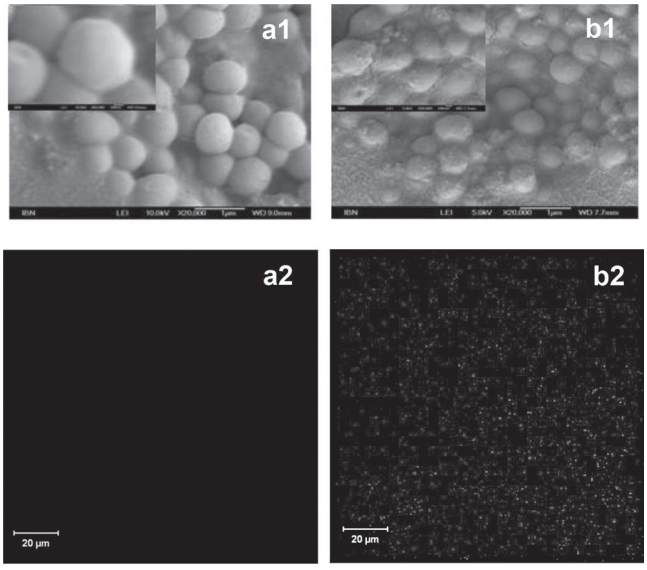

Figure 3. Antimicrobial mechanism studies. a1,b1) SEM images of *S. aureus* 29737 before (a2) and after treatment with 3c at 2×MIC for 2 h (b2) (Inserts: images at higher magnification). Scale bar: 1 μm; a2,b2) Confocal images of *S. aureus* 29737 before (a1) and after treatment with 3c at 2×MIC for 2 h (b1) (PI fluorescence).

3c (**Figure 3**a1,b1). The untreated bacteria showed intact morphology with smooth surfaces. However, the SEM image of *S. aureus* 29737 revealed rough and damaged surfaces after treatment for 2 h at a lethal concentration (2×MIC). Furthermore, the extent of calcein (a fluorescent dye) leakage from calcein-loaded lipid vesicles was used to study the membrane disintegration activity of cationic compounds. Lipid vesicles composed of DOPG: CL (58 : 42) and DOPC (100%) served to mimic the membranes of Gram-positive bacteria and mammalian cells, respectively.[24] As reflected in **Figure 4**a, **3c** caused minimal dye leakage from DOPC lipid vesicles, while it brought about high calcein leakage from the phospholipid vesicles that mimic the Gram-positive membrane in a dose-dependent manner. These results indicated that **3c** was efficient in disintegrating the bacterial membrane mimic with high selectivity. The selectivity is believed to be attributed to the differences in the phospholipid compositions between mammalian and bacterial membranes. The primary phospholipids in the outer leaflet of mammalian cell membranes are zwitterionic phosphatidylcholines (PC). On the other hand, the *S. aureus* membrane is rich in anionic phosphatidylglycerol (PG, 57%) and anionic cardiolipin (43%).[20] Therefore, **3c** interacts preferentially with bacterial membranes over mammalian cell membranes via electrostatic interaction.

In addition, bacterial membrane disruption induced by **3c** was further evaluated with a propidium iodide (PI) permeability assay. As shown in Figure 3a2, no detectable fluorescence was observed in control *S. aureus* without any treatment, implying intact membranes. In contrast, the **3c**-treated *S. aureus* cells showed red fluorescence (Figure 3b2), indicating that PI had intercalated with DNA upon entering the membrane-compromised cells. Interestingly, no FITC-dextran (100 kDa) uptake was observed for both untreated control cells and cells (*S. aureus* 29737) incubated with **3c** at a

DOI: 10.1002/smll.201303921

NANO MICRO small

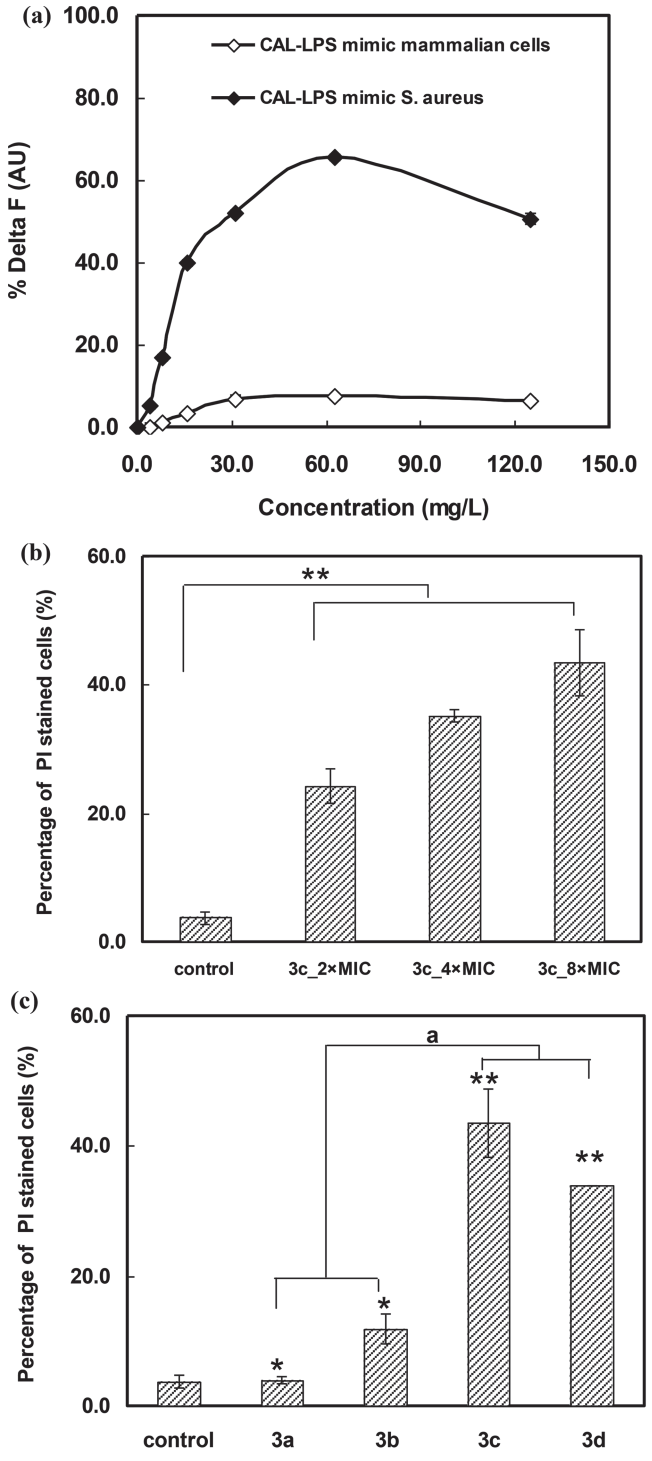

Figure 4. Membrane-lytic property of 3c. a) Calcein leakage from calcein-loaded liposomes (CAL-LPS); (b) Percentage of *S. aureus* 29737 cells stained with PI after incubation with 3c at various concentrations; c) Percentage of *S. aureus* 29737 cells stained with PI after incubation with 3a-3d at 125 mg/L. *$p > 0.05$ versus control; **$p < 0.05$ versus control; a, $p<0.05$, 3a and 3b versus 3c and 3d at 125 mg/L.)

concentration of 2×MIC (data not shown). As there were two size populations in FITC-dextran (100 kDa) conjugate solution (11–58 nm and 68–615 nm), the pore sizes induced by **3c** might be less than 11 nm. The ability of **3c** to disintegrate the membrane of *S. aureus* 29737 (10^8 CFU/mL) was further quantified with PI using flow cytometric analysis. As illustrated in Figure 4b, the control showed only 3.8% PI-positive cells, while the percentage of PI-positive cells in the **3c**-treated group was much higher and dose-dependent (i.e. 24.2%, 35.2% and 41.8% for 2×MIC, 4×MIC and 8×MIC respectively), which further demonstrated that **3c** was able to disintegrate the bacterial membrane. In comparison, **3a-d** with the concentration of 125 mg/L resulted in PI-stained cells of 4.0, 11.9, 41.8 and 33.9%, respectively (Figure 4c), which correlated well with the antimicrobial activity of these cationic compounds (Table 1), e.g. the most potent compound **3c** caused the greatest extent of membrane disruption.

Hemolysis is a major side effect of many cationic antimicrobial peptides and polymers, and the hemolytic activity of our cationic compounds was examined by incubating rat red blood cells (rRBCs) with various concentrations of the antimicrobial agents. As shown in Figure S3, the cationic compounds produced negligible hemolysis even at concentrations up to 1000 mg/L. The selective index (SI, HC_{15}/MIC_{MRSA}) was utilized to assess the selectivity of compounds towards MRSA over mammalian cells, where HC_{15} was defined as the lowest concentration that induces 15% or more hemolysis. All the compounds were found to have high SIs of greater than 10. In particular, **3c** demonstrated excellent selectivity with a SI of 64.1 towards all Gram-positive bacteria tested, including MRSA, due to their potent antimicrobial activity and low hemolytic potential.

In conclusion, a series of novel cationic oligomers of discrete molecular weights have been rationally designed and synthesized. These compounds self-assemble into well-defined nanofibers or spherical nanostructures depending on the nature of the terminal alkyl/aryl substituents. Increasing the hydrophobicity of the terminal group from propyl to hexyl leads to significantly enhanced antimicrobial activity. The compound with the hexyl terminal group formed spherical nanostructures, which showed significant broad-spectrum antimicrobial activity and negligible hemolytic potential. Bacteria did not develop any drug resistance even after multiple sub-lethal dose exposures to the cationic agents due to the physical nature of the antimicrobial mechanism. The cationic oligomers reported herein and the nanostructures derived from them appear promising as antimicrobial agents for the prevention and treatment of multidrug-resistant infections.

Experimental Section

The materials and methods describing the synthesis and self-assembly of cationic compounds, measurement of zeta potential and critical micelle concentration, antimicrobial assay, scanning electron microscopy (SEM), confocal laser scanning microscopy, flow cytometry, dye leakage assay and hemolysis are included in the Supporting Information.

Supporting Information

Supporting Information is available from the Wiley Online Library or from the author.

DOI: 10.1002/smll.201303921

Acknowledgements

The authors would like to acknowledge financial support from the Institute of Bioengineering and Nanotechnology (Biomedical Research Council, Agency for Science, Technology and Research, Singapore) and IBM Almaden Research Center, USA.

[1] a) D. I. Andersson, D. Hughes, *Nat. Rev. Microbiol.* **2010**, *8*, 260; b) K. Bush, P. Courvalin, G. Dantas, J. Davies, B. Eisenstein, P. Huovinen, G. A. Jacoby, R. Kishony, B. N. Kreiswirth, E. Kutter, S. A. Lerner, S. Levy, K. Lewis, O. Lomovskaya, J. H. Miller, S. Mobashery, L. J. V. Piddock, S. Projan, C. M. Thomas, A. Tomasz, P. M. Tulkens, T. R. Walsh, J. D. Watson, J. Witkowski, W. Witte, G. Wright, P. Yeh, H. I. Zgurskaya, *Nat. Rev. Microbiol.* **2011**, *9*, 894.

[2] a) S. E. Cosgrove, Y. L. Qi, K. S. Kaye, S. Harbarth, A. W. Karchmer, Y. Carmeli, *Infect. Control Hosp. Epidemiol.* **2005**, *26*, 166; b) L. B. Rice, *Am. J. Infect. Control* **2006**, *34*, S11.

[3] a) T. R. Pasquale, B. Jabrocki, S. J. Salstrom, T. L. Wiemken, P. Peyrani, N. Z. Haque, E. G. Scerpella, K. D. Ford, M. J. Zervos, J. A. Ramirez, T. M. File, I.-H. S. Grp, *Int. J. Infect. Dis.* **2013**, *17*, E398; b) I. M. Gould, J. Reilly, D. Bunyan, A. Walker, *Clin. Microbiol. Infect.* **2010**, *16*, 1721.

[4] a) R. E. W. Hancock, H. G. Sahl, *Nat. Biotechnol.* **2006**, *24*, 1551; b) Salick, D. A. , J. K. Kretsinger, D. J. Pochan, J. P. Schneider, *J. Am. Chem. Soc.* **2007**, *129*, 14793; c) D. A. Salick, D. J. Pochan, J. P. Schneider, *Adv. Mater.* **2009**, *21*, 4120.

[5] a) M. Zasloff, *Nature* **2002**, *415*, 389; b) N. Wiradharma, S. Q. Liu, Y. Y. Yang, *Small* **2012**, *8*, 362.

[6] a) K. A. Brogden, *Nat. Rev. Microbiol.* **2005**, *3*, 238; b) H. Leontiadou, A. E. Mark, S. J. Marrink, *J. Am. Chem. Soc.* **2006**, *128*, 12156.

[7] A. K. Marr, W. J. Gooderham, R. E. W. Hancock, *Curr. Opin. Pharmacol.* **2006**, *6*, 468.

[8] I. Ivanov, S. Vemparala, V. Pophristic, K. Kuroda, W. F. DeGrado, J. A. McCammon, M. L. Klein, *J. Am. Chem. Soc.* **2006**, *128*, 1778.

[9] K. Kuroda, W. F. DeGrado, *J. Am. Chem. Soc.* **2005**, *127*, 4128.

[10] J. Lin, S. Y. Qiu, K. Lewis, A. M. Klibanov, *Biotechnol. Prog.* **2002**, *18*, 1082.

[11] M. F. Ilker, K. Nusslein, G. N. Tew, E. B. Coughlin, *J. Am. Chem. Soc.* **2004**, *126*, 15870.

[12] B. P. Mowery, S. E. Lee, D. A. Kissounko, R. F. Epand, R. M. Epand, B. Weisblum, S. S. Stahl, S. H. Gellman, *J. Am. Chem. Soc.* **2007**, *129*, 15474.

[13] V. Sambhy, B. R. Peterson, A. Sen, *Angew. Chem. Int. Edit.* **2008**, *47*, 1250.

[14] C. C. Zhou, X. B. Qi, P. Li, W. N. Chen, L. Mouad, M. W. Chang, S. S. J. Leong, M. B. Chan-Park, *Biomacromolecules* **2010**, *11*, 60.

[15] F. Nederberg, Y. Zhang, J. P. K. Tan, K. J. Xu, H. Y. Wang, C. Yang, S. J. Gao, X. D. Guo, K. Fukushima, L. J. Li, J. L. Hedrick, Y. Y. Yang, *Nat. Chem.* **2011**, *3*, 409.

[16] W. Chin, C. Yang, V. W. L. Ng, Y. Huang, J. C. Cheng, Y. W. Tong, D. J. Coady, W. M. Fan, J. L. Hedrick, Y. Y. Yang, *Macromolecules* **2013**, *46*, 8797.

[17] A. C. Engler, J. P. Tan, Z. Y. Ong, D. J. Coady, V. W. Ng, Y. Y. Yang, J. L. Hedrick, *Biomacromolecules* **2013**, *14*, 4331.

[18] a) K. Fukushima, J. P. K. Tan, P. A. Korevaar, Y. Y. Yang, J. Pitera, A. Nelson, H. Maune, D. J. Coady, J. E. Frommer, A. C. Engler, Y. Huang, K. J. Xu, Z. K. Ji, Y. Qiao, W. M. Fan, L. J. Li, N. Wiradharma, E. W. Meijer, J. L. Hedrick, *ACS Nano* **2012**, *6*, 9191; b) K. Fukushima, S. Liu, H. Wu, A. C. Engler, D. J. Coady, H. Maune, J. Pitera, A. Nelson, N. Wiradharma, S. Venkataraman, Y. Huang, W. Fan, J. Y. Ying, Y. Y. Yang, J. L. Hedrick, *Nat. Commun.* **2013**, *4*, 2861.

[19] S. Q. Liu, C. Yang, Y. Huang, X. Ding, Y. Li, W. M. Fan, J. L. Hedrick, Y. Y. Yang, *Adv. Mater.* **2012**, *24*, 6484.

[20] a) S. T. Albelo, C. E. Domenech, *FEMS Microbiol. Lett.* **1997**, *156*, 271; b) K. Lohner, E. J. Prenner, *Biochim. Biophys. Acta Biomembr.* **1999**, *1462*, 141.

[21] L. H. Liu, K. J. Xu, H. Y. Wang, P. K. J. Tan, W. M. Fan, S. S. Venkatraman, L. J. Li, Y. Y. Yang, *Nat. Nanotechnol.* **2009**, *4*, 457.

[22] N. Wiradharma, M. Khan, L. K. Yong, C. A. E. Hauser, S. V. Seow, S. G. Zhang, Y. Y. Yang, *Biomaterials* **2011**, *32*, 9100.

[23] S. Dzidic, J. Suskovic, B. Kos, *Food Technol. Biotechnol.* **2008**, *46*, 11.

[24] S. K. Vooturi, M. B. Dewal, S. M. Firestine, *Org. Biomol. Chem.* **2011**, *9*, 6367.

Received: December 25, 2013
Published online:

DOI: 10.1002/smll.201303921